RL-TR-94-123
In-House Report
September 1994

POLYCRYSTALLINE PLZT/ITO CERAMIC ELECTRO-OPTIC PHASE GRATINGS: ELECTRO-OPTICALLY RECONFIGURABLE DIFFRACTIVE DEVICES FOR FREE-SPACE AND IN-WAFER INTERCONNECTS

Pierre J. Talbot, Joanne H. Maurice

APPROVED FOR PUBLIC RELEASE; DISTRIBUTION UNLIMITED.

Rome Laboratory
Air Force Materiel Command
Griffiss Air Force Base, New York

This report has been reviewed by the Rome Laboratory Public Affairs Office (PA) and is releasable to the National Technical Information Service (NTIS). At NTIS it will be releasable to the general public, including foreign nations.

RL-TR-94-123 has been reviewed and is approved for publication.

APPROVED: James W Cusack

JAMES W. CUSACK, Chief
Photonics & Optics Division
Surveillance & Photonics Directorate

FOR THE COMMANDER: Luke L Lucas

LUKE L. LUCAS, Colonel, USAF
Deputy Director
Surveillance & Photonics Directorate

If your address has changed or if you wish to be removed from the Rome Laboratory mailing list, or if the addressee is no longer employed by your organization, please notify RL (OCPB) Griffiss AFB NY 13441. This will assist us in maintaining a current mailing list.

Do not return copies of this report unless contractual obligations or notices on a specific document require that it be returned.

REPORT DOCUMENTATION PAGE

Form Approved
OMB No. 0704-0188

1. AGENCY USE ONLY (Leave Blank)	2. REPORT DATE	3. REPORT TYPE AND DATES COVERED
	September 1994	In-House Oct 92 - Sep 93

4. TITLE AND SUBTITLE POLYCRYSTALLINE PLZT/ITO CERAMIC ELECTRO-OPTIC PHASE GRATINGS: ELECTRO-OPTICALLY RECONFIGURABLE DIFFRACTIVE DEVICES FOR FREE-SPACE AND IN-WAFER INTERCONNECTS

5. FUNDING NUMBERS
PE - 62702F
PR - 4600
TA - P3
WU - 25

6. AUTHOR(S)
Pierre J. Talbot, Joanne H. Maurice

7. PERFORMING ORGANIZATION NAME(S) AND ADDRESS(ES)
Rome Laboratory (OCPB)
25 Electronic Pky
Griffiss AFB NY 13441-4515

8. PERFORMING ORGANIZATION REPORT NUMBER
RL-TR-94-123

9. SPONSORING/MONITORING AGENCY NAME(S) AND ADDRESS(ES)
Rome Laboratory (OCPB)
25 Electronic Pky
Griffiss AFB NY 13441-4515

10. SPONSORING/MONITORING AGENCY REPORT NUMBER

11. SUPPLEMENTARY NOTES
Rome Laboratory Project Engineer: Joanne H. Maurice/OCPB (315) 330-7670

12a. DISTRIBUTION/AVAILABILITY STATEMENT
Approved for public release; distribution unlimited.

12b. DISTRIBUTION CODE

13. ABSTRACT (Maximum 200 words)

The potential of electro-optically reconfigurable phase-only diffractive devices as a suitable extension to static diffractive elements for optical free-space and waveguide interconnects is investigated through the fabrication, testing and modeling of polycrystalline PLZT/ITO ceramic electro-optic phase-only gratings.

14. SUBJECT TERMS PLZT Diffraction Grating, Electro-Optic Diffraction Grating, Optical Switching, Optical Interconnects, Reconfigurable Interconnect

15. NUMBER OF PAGES 44

16. PRICE CODE

17. SECURITY CLASSIFICATION OF REPORT	18. SECURITY CLASSIFICATION OF THIS PAGE	19. SECURITY CLASSIFICATION OF ABSTRACT	20. LIMITATION OF ABSTRACT
UNCLASSIFIED	UNCLASSIFIED	UNCLASSIFIED	U/L

NSN 7540-01-280-5500

Standard Form 298 (Rev. 2-89)
Prescribed by ANSI Std. Z39-18
298-102

Acknowledgments

We thank Dr. Q. Wang Song of the Electrical and Computer Engineering Department, Syracuse University, and Paul R. Cook, Jacqueline D. Smith, and Captain Edward N. Toughlian of the Photonics Center of Rome Laboratory for their technical assistance. We acknowledge the generous support of Mr. Hank Burke of Motorola Ceramics. Dr. Richard J. Michalak, as director of the Digital Photonics Branch, made available the laboratory and computer facilities of the Photonic Center of Rome Laboratory.

This work was performed in part at the National Nanofabrication Facility which is supported by the National Science Foundation under Grant ECS-8619049, Cornell University and industrial affiliates.

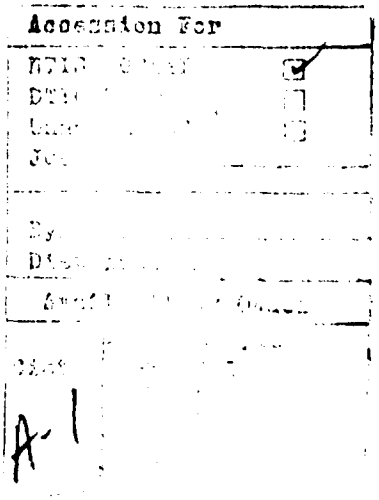

Table of Contents

Abstract ii

Acknowledgments iii

Table of Contents iv

1. Introduction 1

2. Design and Fabrication 4

3. Experimental Results 6

4. Theoretical Model 12

5. Simulation Results 20

6. Conclusions 28

References 30

1. Introduction

Substantial modeling and analysis has been conducted which convincingly presents the advantages of optical interconnections over electronic interconnections in electronics processors for chip-to-chip and board-to-board communications [1,2,3,4]. Extensive research continues in both guided-wave and free-space implementations of optical interconnection architectures [5-12]. Optical-interconnect architectures are based on static and dynamically reconfigurable interconnection element schemes. The static interconnection schemes utilize predominately fixed-index-profile diffractive elements or holographic-gelatin diffractive elements. The dynamically-reconfigurable interconnection schemes are based primarily on spatial light modulators or photorefractive elements.

In all of these interconnection architectures the optical interconnection pathway is established and determined by the orientations of the optical "source" and "detector," with the interconnection element simply acting to guide the optical communication through fixed waveguide or free-space pathways. In the dynamic interconnection schemes, a pathway may or may not be utilized in a particular processing step; but all the virtual optical interconnection pathways are determined by the source-detector pairs in the particular architecture. The source-detector pair determination of optical pathways common to these interconnection architectures implies the proportional growth of the number of sources with optical interconnection density. In the architectures referenced, the number of detectors would also grow proportionally with the interconnection density.

Critical problems in implementing a high-density optical-interconnect architecture include fabrication alignment tolerances, post-fabrication alignment, source and/or detector failures. A new interconnection strategy is required in order to relax the tolerance constraints imposed on high-density optical-interconnect architectures. Optical pathways within an interconnect architecture should be established and reconfigured at interconnection elements linking the sources and detectors rather than by the orientation of source-detector pairs within the architecture. An architectural strategy based on this would require such elements to be locally-controllable with discrete or continuous scanning functionality.

We propose PLZT (lead lanthanum zirconate titanate)/ITO (indium tin oxide) electro-optic phase-only micro-optic structures as a candidate technology to implement

reconfigurable index profile (RIP) diffractive elements for optical-interconnect architectures. Here we report on the potential application of RIP diffractive optical interconnection elements as determined by our fabrication, evaluation, and modeling of polycrystalline PLZT/ITO ceramic electro-optic phase gratings.

Electro-optic materials have been extensively researched and utilized in spatial light modulator and deflector schemes. Lithium niobate ($LiNbO_3$) and PLZT-ceramic compositions have been investigated in applications as both bulk material modulators and deflectors as well as epitaxial thin-film integrated optoelectronic structures. Modulator and deflector schemes are primarily based on birefringence-induced polarization rotation or various electrode-array-based diffractive effects.

Electro-optic materials are typically utilized in modulation schemes. The electro-optic properties of the material affect a rotation in the polarization of the incident optical beam. The beam is introduced to the electro-optic material such that the electric-field vector is oriented 45 degrees from both the directions of ordinary and extraordinary refractive indices. This affects a rotation in polarization through the birefringence induced in the electro-optic material. The electro-optic polarization rotation is exploited to produce an electro-optic modulator by sandwiching the electro-optic material between a pair of fixed polarizers/analyzers oriented such that their directions of preferred polarization are crossed (perpendicular), while the orientation of the polarizer is parallel to the electric-field vector of the incident beam (Figure 1.1). Bulk electro-optic modulators based on this scheme exhibit stringent requirements regarding the alignment tolerances of the beam and the polarization orientations. These requirements, in turn, impose limits on the modulator field of view [13]. Also, large modulator apertures require prohibitively high voltages. And, due to temperature sensitivity of the electro-optic effect, the rotation schemes require cooling for stable operation.

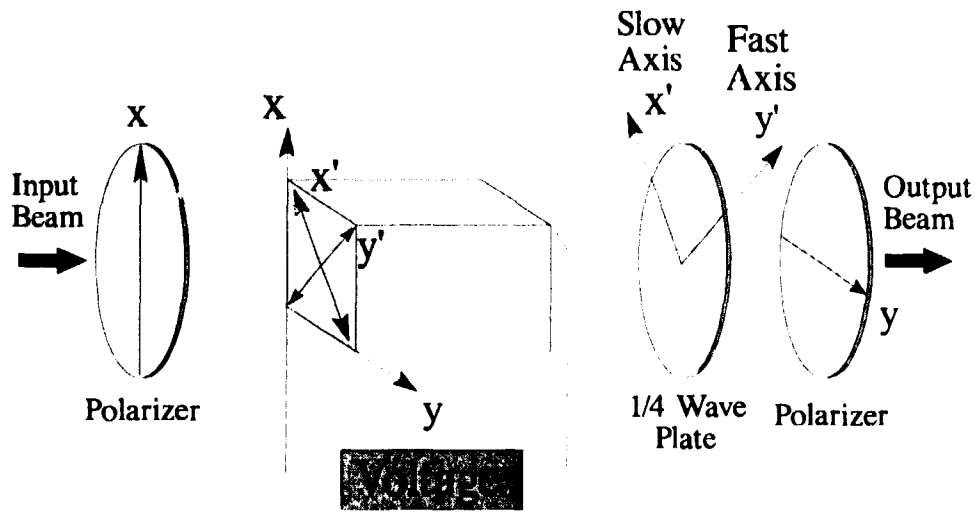

Figure 1.1 Typical scheme for electro-optic amplitude modulator.

A number of electro-optic modulator-array-based schemes employing electrode gratings have been reported utilizing the linear electro-optic effect in LiNbO3. The majority of the devices operate as waveguide structures to affect an increase in the interaction length of the electro-optic effect for the purpose of reducing the required voltages [14-19]. The relatively long interaction lengths required suggest waveguide-based structures are incompatible with integrated optoelectronics as well as being unsuitable for free-space optical interconnection. A promising diffraction-based modulator employing LiNbO3 has been reported [13]. The diffraction modulator is operated in a transmissive mode as a thin optical flat suggesting potential application in free-space architectures. The voltages required for its operation, however, are in the kilovolts range.

In all these devices, the use of LiNbO3 hampers the device design, fabrication, and operation that is most compatible with microelectronics. This is due to the crystal's electro-optic tensor, which requires a certain crystal orientation and alignment, and the crystal's intrinsic birefringence. LiNbO3's electro-optic tensor limits designs to uniform electric fields configured so as not to cause rotations of the principle axis of the refractive-index ellipsoid, as otherwise complex circular polarizations are produced. The material's linear electro-optic behavior requires larger operating voltages than comparable quadratic electro-optic materials. The intrinsic birefringence of LiNbO3 dictates the polarization orientation of optical beams traveling through it. In addition, LiNbO3 suffers from optical power limitations due to optical damage induced by the photorefractive effect .

Attempts to produce devices that utilize the electro-optic-induced change in a specific refractive index are less common [20-25]. Reflective electro-optic PLZT gratings have been reported. The diffractive performance of the gratings, however is poor. Far better results have been reported for an electro-optic PLZT variable-focal-length lens and electro-optic PLZT dual-focal-length Fresnel lens.

Electro-optic PLZT compositions hold promise for the development of RIP diffractive elements for optical-interconnect architectures. To demonstrate this potential, we have designed and fabricated a polycrystalline PLZT/ITO ceramic electro-optic phase-only grating. The experimental investigation and theoretical analysis of the diffractive performance of our electro-optic phase grating documents the potential of electro-optical RIP diffractive optics. Our PLZT electro-optic phase grating demonstrates significant improvements and advantages in performance over previously-reported bulk modulators and deflectors that utilize either LiNbO3 or PLZT. In addition, the theoretical model we develop explains the insignificant diffractive efficiencies reported for previous designs of PLZT electro-optic diffraction gratings. Our model also suggests polycrystalline PLZT ceramic electro-optic design principles that would significantly improve the design and performance of the previously-reported PLZT electro-optic lens structures.

2. Design and Fabrication

The polycrystalline PLZT/ITO ceramic electro-optic phase grating consists of a transparent indium tin oxide (ITO) interdigital electrode grating fabricated upon a transparent optically-polished wafer of lead lanthanum zirconate titanate (PLZT) ceramic (Figure 2.1). Thin films of ITO are applied to PLZT ceramic wafers through magnetron sputter deposition. The thin films exhibit an 89% transmission for visible frequencies at a resistivity of 25 Ohms/sq. at a deposition depth of 1450 angstroms. PLZT ceramic composition determines wafer transparency and the material's electro-optic behavior. PLZT composition is denoted by a (y/z/1-z) notation, where y is the percentage of lead sites occupied by lanthanum, and z/1-z is the zirconate-to-titanate ratio in the material. Lanthanum concentration determines the transparency of the PLZT ceramic. Lanthanum concentration coupled with the zirconate-titanate ratio determines the electro-optic behavior of the PLZT ceramic. The polycrystalline PLZT (9.5/65/35) ceramic wafer is of a

quadratic electro-optic composition and exhibits 65% transmission for visible and infrared frequencies. PLZT (9.5/65/35) ceramic possesses no intrinsic birefringence and its electro-optic behavior exhibits no significant hysteresis [26-28]. PLZT ceramic wafers of 12.5 mils thickness were cut and polished from dense hot-pressed cylindrical blocks.

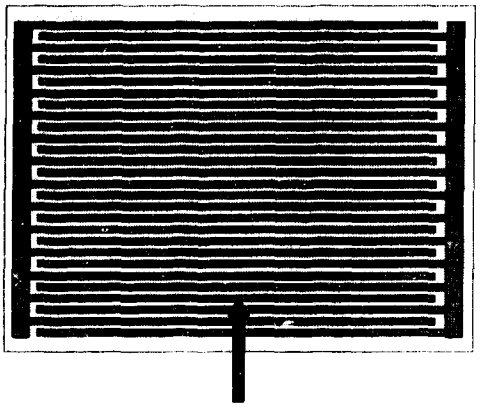

Figure 2.1 Polycrystalline PLZT/ITO ceramic electro-optic phase grating

The lines and spaces of the ITO electrode grating have a 100 um width for a grating period of 200 um. The ITO electrode grating's dimension is one square centimeter. The ITO electrode grating thin-film pattern can be transferred either through a subtractive argon-ion sputter etch of the ITO thin film or an additive ITO deposition and lift-off process. ITO electrode gratings were produced through both processes. The dimensions of our initial gratings were selected to accommodate meaningful performance comparisons with previously-reported devices.

The polycrystalline PLZT/ITO ceramic electro-optic phase grating consists of an intrinsic phase grating due to the transparent ITO electrode grating and an electro-optically-induced phase grating within the PLZT ceramic wafer produced by the electric field applied through the ITO electrode grating. Unlike the previously reported electro-optic grating [20], which fails to demonstrate significant reconfigurable diffractive efficiency, our design utilizes transparent ITO electrodes to produce a true phase-only diffraction grating. In addition, the design of previously-reported electro-optic gratings incorporates a ground plane which establishes applied electric fields normal to the PLZT wafer surfaces. Our subsequent analysis will show that normal electric fields induce insignificant index profile grating for both parallel- and perpendicularly-oriented optical

plane waves by coupling through the off-diagonal Kerr coefficients of the quadratic electro-optic tensor. Our polycrystalline PLZT/ITO ceramic electro-optic phase grating, by correcting these design errors, demonstrates significant reconfigurable phase-grating diffraction efficiencies.

3. Experimental Results

The performance of the polycrystalline PLZT/ITO ceramic electro-optic phase-grating is characterized as a potential reconfigurable transmissive and reflective diffractive element through an examination of the phase grating's Fresnel diffraction pattern under static applied voltage (Figure3.1). The PLZT/ITO electro-optic phase grating is mounted such that the surface of the wafer with the deposited transparent ITO electrode grating faces the transmitted Fresnel diffraction pattern. All reported transmitted and reflected Fresnel diffraction patterns correspond to a plane-wave source beam whose electric-field vector is oriented perpendicular to the digits of the ITO electrode grating. The Fresnel diffraction patterns corresponding to a plane-wave source beam parallel to the digits of the ITO electrode grating showed no significant variation under applied voltage from that produced by the intrinsic ITO electrode phase grating. The electro-optically-induced phase grating within the PLZT wafer is insignificant for a plane wave source beam with an electric-field vector oriented parallel to the ITO electrode grating.

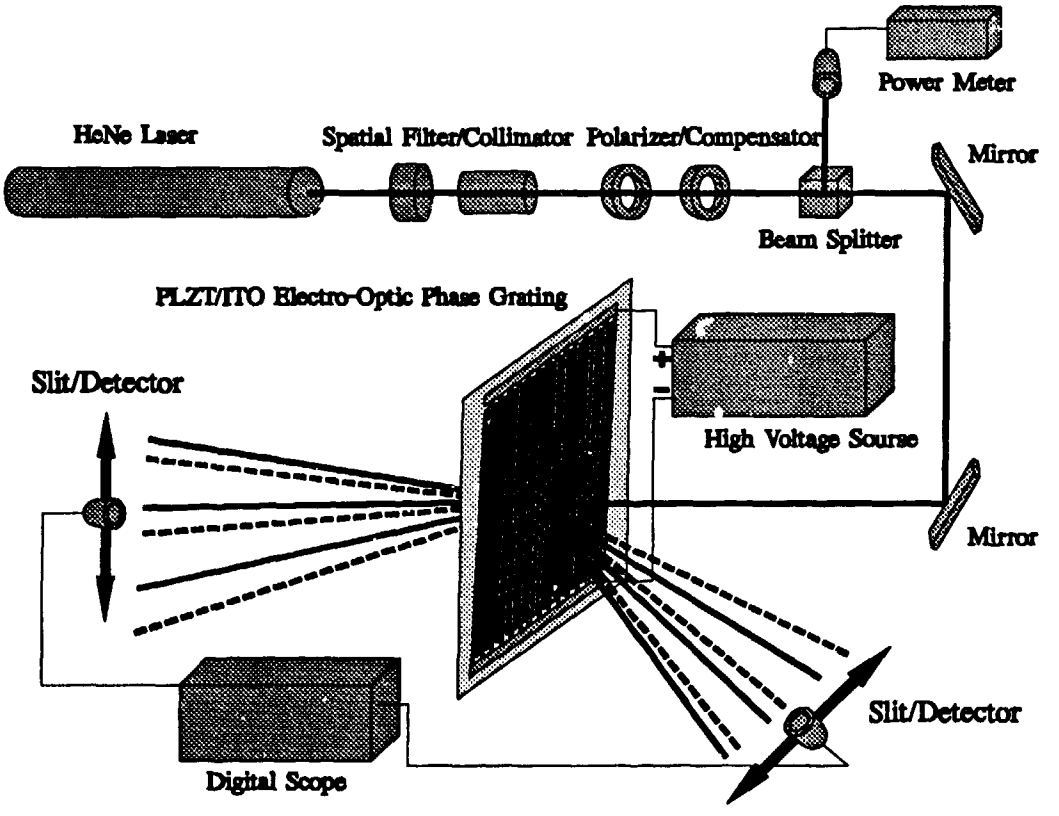

Figure 3.1 Experimental setup for recording transmitted and reflected Fresnel diffraction patterns.

The transmitted Fresnel diffraction pattern of the PLZT/ITO electro-optic phase grating with zero applied voltage is simply that expected from the intrinsic relief phase grating due to the transparent ITO electrode grating (Figure 3.2a). The reflected Fresnel diffraction pattern with zero applied voltage is insignificant and consists essentially of the portion of the source beam reflected according to Fresnel reflection and transmission laws.

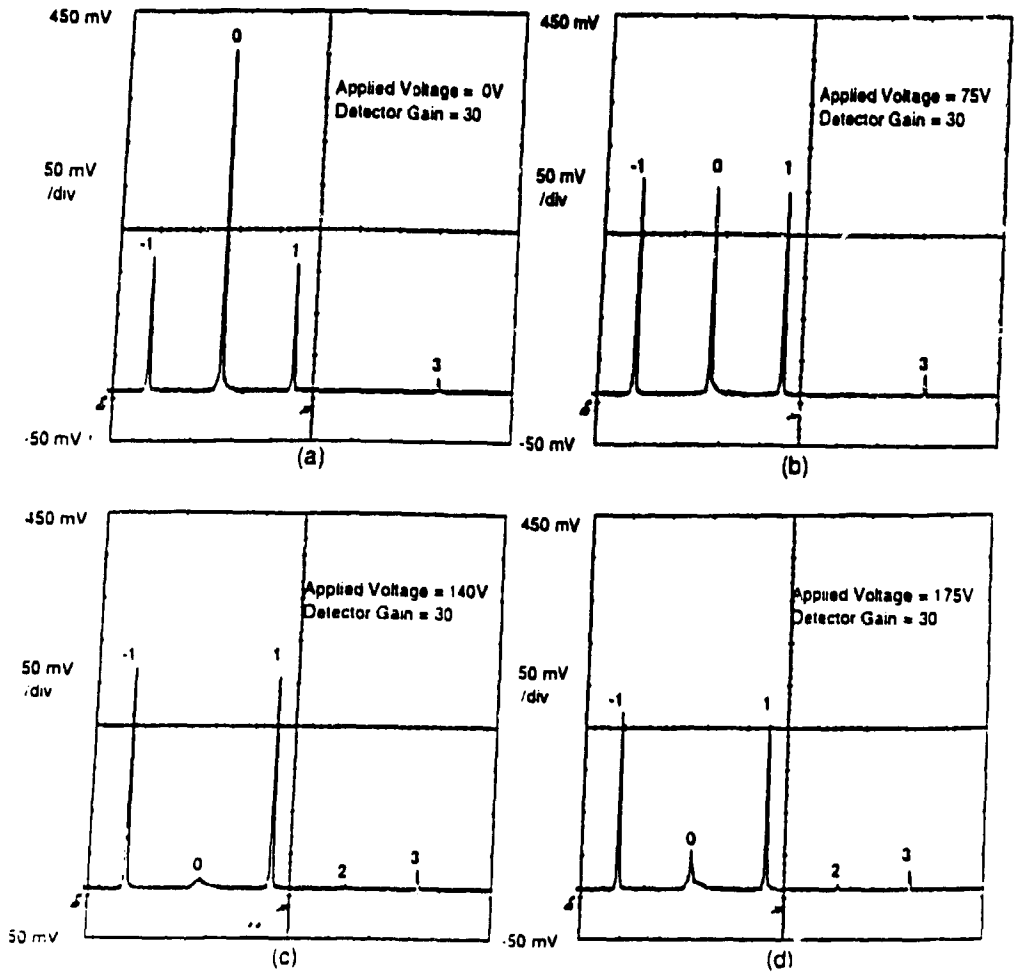

Figure 3.2 Transmitted Fresnel diffraction pattern due to electro-optic PLZT/ITO phase grating for perpendicular polarization :
a) intrinsic ITO electrode phase grating (i.e., v=0V)
b) v=75V, c) v=140V, d) v=175V

The transmitted Fresnel diffraction pattern at a sequence of applied voltages documents a number of features observed in the performance of the PLZT/ITO electro-optic phase grating (Figure 3.2). First, the intrinsic Fresnel diffraction pattern possesses only odd higher-order modes. Secondly, the power of the zero-order mode of the pattern is switched almost entirely into higher-order modes in a continuous manner. Thirdly, even-order modes appear and continuously increase. Finally, increasing the applied voltage past the zero-order mode switch-off voltage of 140V results in the return of the zero-order mode without a decrease in any of the higher-order modes. In fact, the even-order modes increase still further. The behavior of the higher-order transmitted modes are

more clearly illustrated in a second set of transmitted Fresnel diffraction patterns under the same sequence of applied voltages (Figure 3.3).

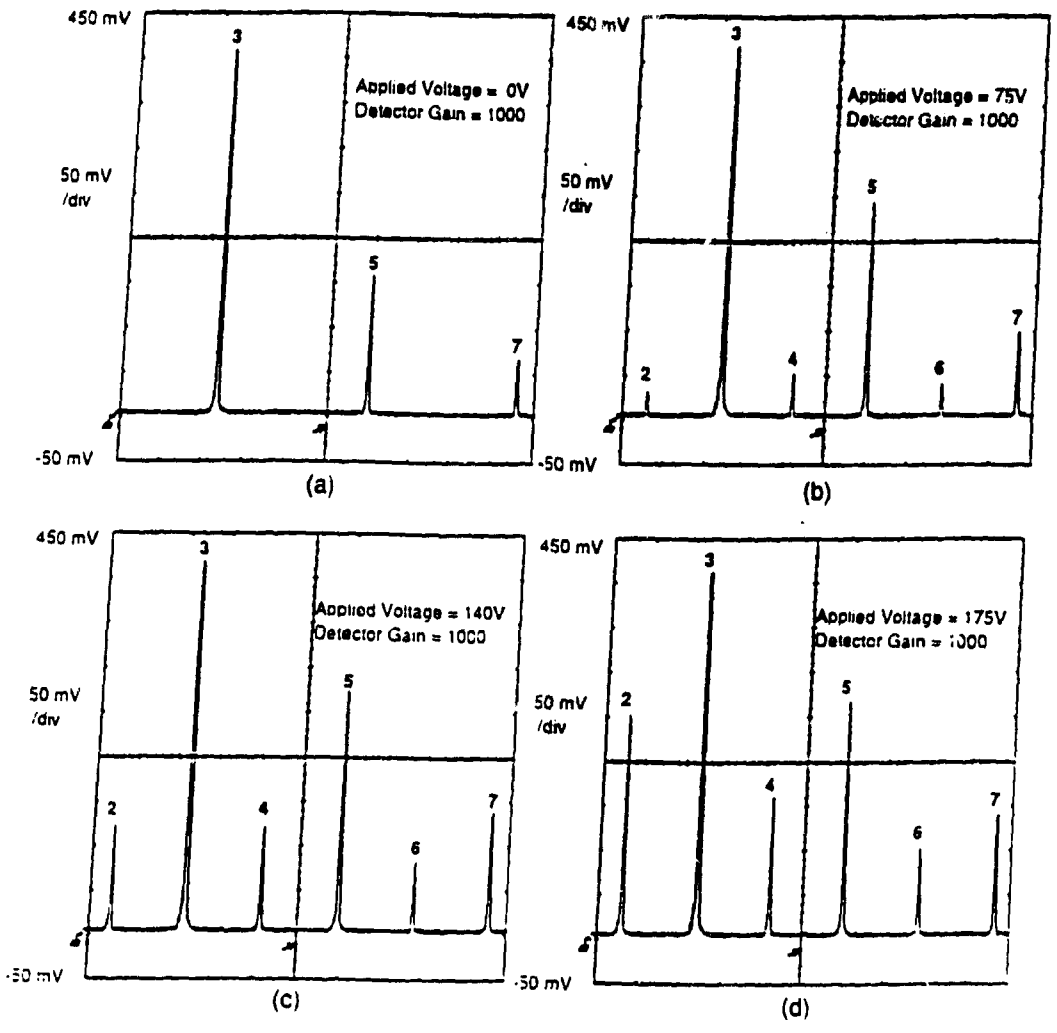

Figure 3.3 Transmitted Fresnel diffraction pattern due to electro-optic PLZT/ITO phase grating for perpendicular polarization - 2nd and higher order modes :
a) intrinsic ITO electrode phase grating (i.e. ,v=0V)
b) v=75V, c) v=140V, d) v=175V

The reflected Fresnel diffraction patterns of the PLZT/ITO electro-optic phase grating for the sequence of applied voltages illustrate some interesting behavior (Figure

3.4, 3.5). Even and odd higher-order modes appear and continuously increase up to the transmitted zero-order mode switch-off voltage of 140V. Subsequent increases in applied voltage past 140V result in the increase of even-order modes and the decrease of odd-order modes. The reflected first-order mode can be switched on and off at 140V and 175V respectively. The decrease in reflected even-order modes past the transmitted zero-order mode switch-off voltage supplies the power for the transmitted zero-order mode's increase past 140V.

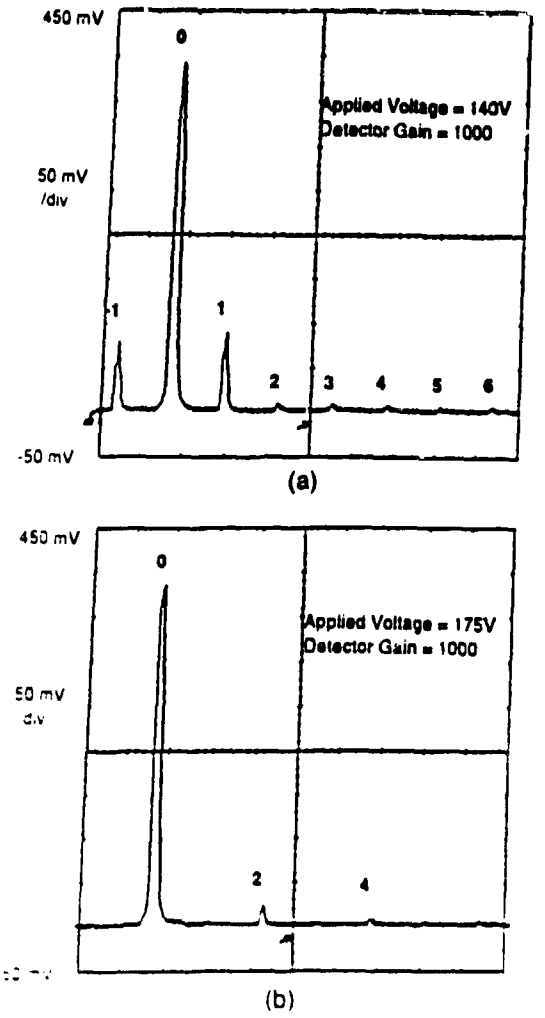

Figure 3.4 Reflected Fresnel diffraction pattern due to electro-optic PLZT/ITO phase grating for perpendicular polarization : a) v=140V, b) v=175V

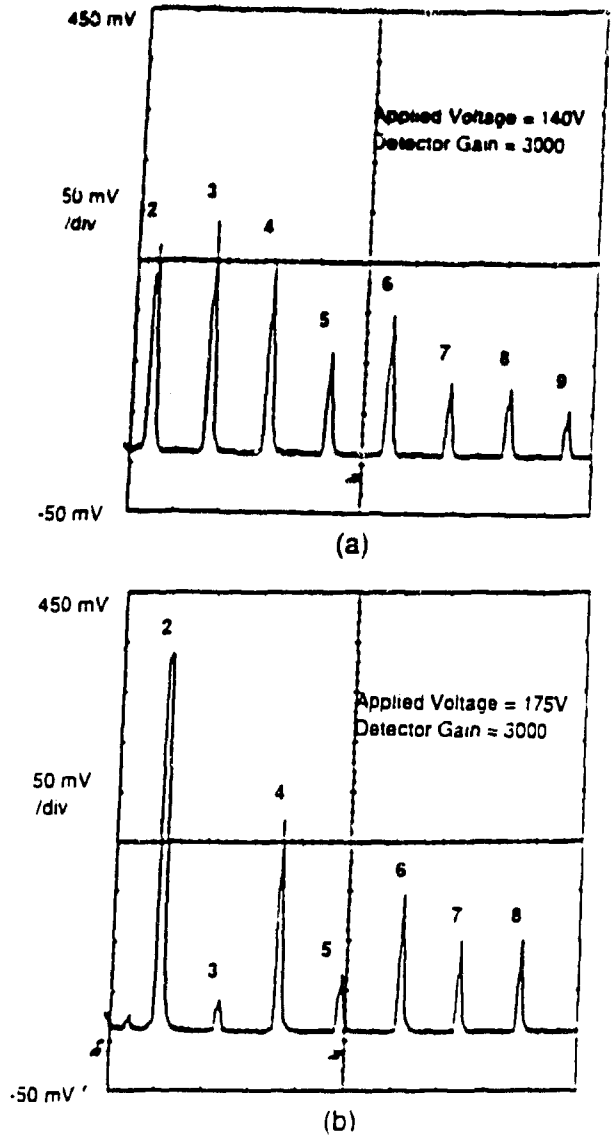

Figure 3.5 Reflected Fresnel diffraction pattern due to electro-optic PLZT/ITO phase grating for perpendicular polarization - 2nd and higher-order modes : a) v=140V, b) v=175V

As expected in utilizing quadratic PLZT (9.5/65/35) ceramic in the electro-optic phase grating, the lack of hysteresis resulted in no observable residual induced phase grating. The reflected and transmitted Fresnel diffraction patterns observed under the sequence of applied voltages were repeatable.

4. Theoretical Model

The polycrystalline PLZT/ITO phase-only diffraction grating previously described and experimentally characterized can be modeled as the superposition of an intrinsic and static phase grating due to the periodic transparent ITO electrode grating and an electro-optically induced and configurable phase grating due to the quadratic electro-optic response of the polycrystalline PLZT ceramic wafer. The ITO electrode grating impresses a periodic electric field distribution within the dielectric PLZT wafer resulting in a period distribution of the refractive index in the PLZT wafer due to the Kerr coefficients of the polycrystalline PLZT ceramic. The electro-optically induced refractive index grating within the transparent PLZT ceramic wafer constitutes a configurable phase grating.

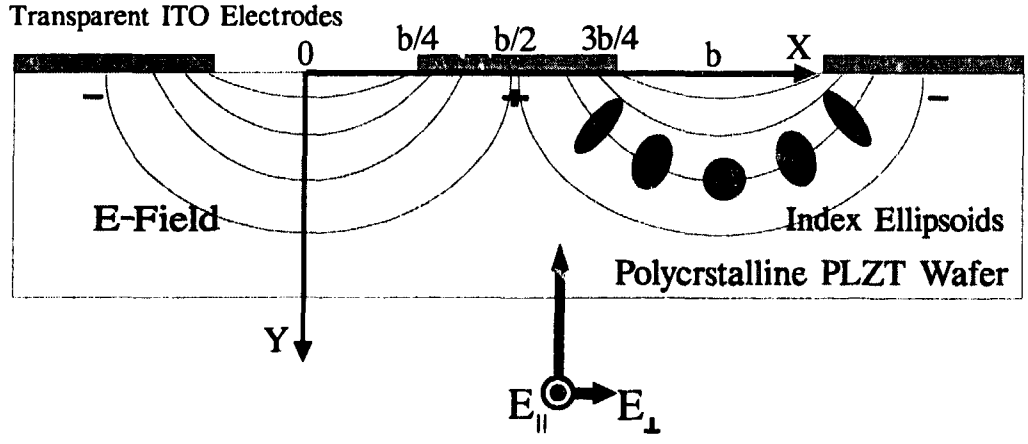

Figure 4.1 Cross section of electro-optic PLZT/ITO Phase grating.

The periodic structure of the transparent ITO electrode grating fabricated upon the PLZT ceramic wafer allows the calculation of the periodic electric field impressed within the PLZT wafer as a closed-form solution to a simple boundary-value problem in the electric potential (Figure 4.1). The solution for the electric potential can be expressed as a period sum.

$$V(x,y) = \sum_{m=1}^{\infty} B_m \sin\left(\frac{m\pi x}{b}\right) e^{-m\pi y / b} \qquad (4.1)$$

The potential is assumed to satisfy an ideal linear boundary condition.

$$V_0(x,0) = \begin{cases} -\dfrac{vx/2}{b/4} & 0 \le x \bmod(2b) \le b/4 \\ -\dfrac{v}{2} & b/4 \le x \bmod(2b) \le 3b/4 \\ -\dfrac{v}{2} + (\dfrac{v/2}{b/4})(x - \dfrac{3b}{4}) & 3b/4 \le x \bmod(2b) \le 5b/4 \\ \dfrac{v}{2} & 5b/4 \le x \bmod(2b) \le 7b/4 \\ \dfrac{v}{2} - (\dfrac{v/2}{b/4})(x - \dfrac{7b}{4}) & 7b/4 \le x \bmod(2b) \le 2b \end{cases} \tag{4.2}$$

The coefficients of the periodic sum are computed as sine transforms.

$$B_m = \frac{1}{b}\int_0^{2b} V_0(x,0)\sin(\frac{m\pi\, x}{b})dx \tag{4.3}$$

The electric field is computed as the gradient of the electric potential.

$$E = -\nabla V \tag{4.4a}$$

$$E_x(x,y) = -\sum_{m=1}^{\infty} B_m(\frac{m\pi}{b})\cos(\frac{m\pi\, x}{b})e^{-m\pi\, y/b} \tag{4.4b}$$

$$E_y(x,y) = \sum_{m=1}^{\infty} B_m(\frac{m\pi}{b})\sin(\frac{m\pi\, x}{b})e^{-m\pi\, y/b} \tag{4.4c}$$

$$E(x,y) = \sqrt{E_x^2(x,y) + E_y^2(x,y)} \tag{4.4d}$$

The polycrystalline PLZT (9.5/65/35) ceramic wafer is of a quadratic electro-optic composition. PLZT (9.5/65/35) ceramic under an applied electric field exhibits a transition from an optically-isotropic cubic phase to a rhombohedral or tetragonal ferroelectric phase with a quadratic optical anisotropy. The induced quadratic optical anisotropy is uniaxial with the optical axis oriented parallel to the applied electric field [26-28]. The electro-optic analysis of the induced phase grating within the PLZT ceramic

wafer is most conveniently conducted utilizing the conception and notation of the index ellipsoid [29-30].

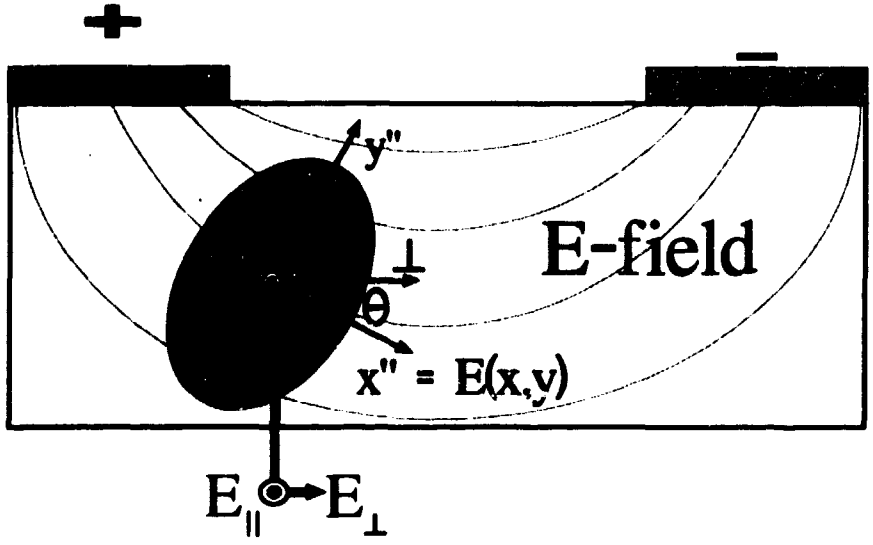

Figure 4.2 Index ellipsoid for PLZT ceramic.

The index ellipsoid for a uniaxial crystal is an ellipse of revolution that characterizes the refractive index experience by an arbitrary optical plane wave in an electro-optic material. (Figure 4.2). For each location within the PLZT ceramic wafer specified through a physical coordinate system, the equation of the index ellipsoid under an applied electric field can be represented in the principle coordinate system of the PLZT ceramic. The principle coordinate system for an electro-optic material corresponds to the orthogonal directions for which the electric-field vector and the electric-flux-density vector of an optical plane wave are parallel.

$$\left(\frac{1}{n_1^2(x,y)}\right)x'^2+\left(\frac{1}{n_2^2(x,y)}\right)y'^2+\left(\frac{1}{n_3^2(x,y)}\right)z'^2+\left(\frac{1}{n_4^2(x,y)}\right)y'z'+\left(\frac{1}{n_5^2(x,y)}\right)z'x'+\left(\frac{1}{n_6^2(x,y)}\right)x'y'=1 \qquad (4.5a)$$

In general, the application of an electric field changes the dimensions and orientation of the index ellipsoid from its unperturbed state. With zero applied electric field the index ellipsoid represented in the principle coordinate system specifies the

refractive index experienced by a plane optical wave with its electric-field vector oriented parallel to one of the principle axes of the ellipsoid.

$$\left(\frac{1}{n_{x'}^2(x,y)}\right)x'^2+\left(\frac{1}{n_{y'}^2(x,y)}\right)y'^2+\left(\frac{1}{n_{z'}^2(x,y)}\right)z'^2=1 \qquad (4.5b)$$

The isotropic nature of quadratic PLZT (9.5/65/35) allows the principle axes of the index ellipsoid to correspond to the physical coordinate system of the wafer.

$$\left(\frac{1}{n_1^2(x,y)}\right)x^2+\left(\frac{1}{n_2^2(x,y)}\right)y^2+\left(\frac{1}{n_3^2(x,y)}\right)z^2+\left(\frac{1}{n_4^2(x,y)}\right)yz+\left(\frac{1}{n_5^2(x,y)}\right)zx+\left(\frac{1}{n_6^2(x,y)}\right)xy=1$$

(4.6a)

The lack of intrinsic birefringence in PLZT (9.5/65/35) makes the unperturbed index ellipsoid particularly simple.

$$\left(\frac{1}{n_o^2}\right)x^2+\left(\frac{1}{n_o^2}\right)y^2+\left(\frac{1}{n_o^2}\right)z^2= \qquad (4.6b)$$

$$\left(\frac{1}{n_1^2(x,y)}\right)\Big|_{E=0}=\frac{1}{n_x^2(x,y)}=\frac{1}{n_o^2} \qquad (4.6c)$$

$$\left(\frac{1}{n_2^2(x,y)}\right)\Big|_{E=0}=\frac{1}{n_y^2(x,y)}=\frac{1}{n_o^2}$$

(4.6d)

$$\left(\frac{1}{n_3^2(x,y)}\right)\Big|_{E=0}=\frac{1}{n_z^2(x,y)}=\frac{1}{n_o^2}$$

(4.6e)

$$\left(\frac{1}{n_4^2(x,y)}\right)\Big|_{E=0}=\left(\frac{1}{n_5^2(x,y)}\right)\Big|_{E=0}=\left(\frac{1}{n_6^2(x,y)}\right)\Big|_{E=0}=0 \qquad (4.6f)$$

The characterization of the refractive index experienced by an arbitrary optical plane wave under an applied electric field is accomplished by determining a coordinate system that reduces the perturbed index ellipsoid to a form possessing no cross terms.

$$\left(\frac{1}{n_{x''}^2(x,y)}\right)x''^2+\left(\frac{1}{n_{y''}^2(x,y)}\right)y''^2+\left(\frac{1}{n_{z''}^2(x,y)}\right)z''^2=1 \qquad (4.7)$$

In general, a non-trivial eigenvalue and eigenfunction computation is required to determine the coordinate system of the reduced form; however, for PLZT (9.5/65/35) ceramic the computation of the physical situation is considerably simplified. The electro-optically induced perturbation in the index ellipsoid of PLZT (9.5/65/35) is characterized by an isotropic quadratic electro-optic tensor equation.

$$\begin{bmatrix} \Delta\left(\frac{1}{n^2(x,y)}\right)_1 \\ \Delta\left(\frac{1}{n^2(x,y)}\right)_2 \\ \Delta\left(\frac{1}{n^2(x,y)}\right)_3 \\ \Delta\left(\frac{1}{n^2(x,y)}\right)_4 \\ \Delta\left(\frac{1}{n^2(x,y)}\right)_5 \\ \Delta\left(\frac{1}{n^2(x,y)}\right)_6 \end{bmatrix} = \begin{bmatrix} R_{11} & R_{12} & R_{12} & 0 & 0 & 0 \\ R_{12} & R_{11} & R_{12} & 0 & 0 & 0 \\ R_{12} & R_{12} & R_{11} & 0 & 0 & 0 \\ 0 & 0 & 0 & \frac{1}{2}(R_{11}-R_{12}) & 0 & 0 \\ 0 & 0 & 0 & 0 & \frac{1}{2}(R_{11}-R_{12}) & 0 \\ 0 & 0 & 0 & 0 & 0 & \frac{1}{2}(R_{11}-R_{12}) \end{bmatrix} \begin{bmatrix} E_x^2(x,y) \\ E_y^2(x,y) \\ E_z^2(x,y) \\ E_y(x,y)E_z(x,y) \\ E_z(x,y)E_x(x,y) \\ E_x(x,y)E_y(x,y) \end{bmatrix}$$

(4.8a)

The optical axis of the uniaxial phase of PLZT (9.5/65/35) under an applied electric field is oriented parallel to the electric field. The coordinate system of the reduced form of the index ellipsoid corresponds to an orthogonal coordinate system oriented so that one of the axes is parallel to the applied electric field. The perturbations to the refractive index under the applied electric field are then simply represented.

$$\begin{bmatrix} \Delta(\frac{1}{n^2(x,y)})_1 \\ \Delta(\frac{1}{n^2(x,y)})_2 \\ \Delta(\frac{1}{n^2(x,y)})_3 \end{bmatrix} = \begin{bmatrix} R_{11} \\ R_{12} \\ R_{12} \end{bmatrix} \left[E^2(x,y)\right] \tag{4.8b}$$

$$(\frac{1}{n^2_{x''}(x,y)}) = (\frac{1}{n^2_x(x,y)}) + R_{11}E^2(x,y) = (\frac{1}{n^2_o}) + R_{11}E^2(x,y) \tag{4.9a}$$

$$(\frac{1}{n^2_{y''}(x,y)}) = (\frac{1}{n^2_y(x,y)}) + R_{12}E^2(x,y) = (\frac{1}{n^2_o}) + R_{12}E^2(x,y) \tag{4.9b}$$

$$(\frac{1}{n^2_{z''}(x,y)}) = (\frac{1}{n^2_z(x,y)}) + R_{12}E^2(x,y) = (\frac{1}{n^2_o}) + R_{12}E^2(x,y) \tag{4.9c}$$

The reduced form of the index ellipsoid is acquired without an eigenvalue and eigenfunction computation. The major axis of the reduced index ellipsoid coincides with the electric-field vector and the remaining axis can be chosen flexibly as any two orthogonal directions in the plane normal to the major axis of the index ellipsoid.

$$\left((\frac{1}{n^2_o}) + R_{11}E^2(x,y)\right)x''^2 + \left((\frac{1}{n^2_o}) + R_{12}E^2(x,y)\right)y''^2 + \left((\frac{1}{n^2_o}) + R_{12}E^2(x,y)\right)z''^2 = 1 \tag{4.10}$$

The refractive index along these axes may be computed.

$$n_{x'}(x,y) = n_o - \frac{1}{2}n_o^3 R_{11}E^2(x,y) \tag{4.11a}$$

$$n_{y'}(x,y) = n_o - \frac{1}{2}n_o^3 R_{12}E^2(x,y) \tag{4.11b}$$

$$n_{z'}(x,y) = n_O - \frac{1}{2} n_O^3 R_{12} E^2(x,y) \qquad (4.11c)$$

Ordinary and extraordinary refractive indexes for the uniaxial phase may be defined.

$$n_{e'}(x,y) = n_{x'}(x,y) \qquad (4.12a)$$

$$n_{O'}(x,y) = n_{y'}(x,y) = n_{z'}(x,y) \qquad (4.12b)$$

$$n_{e'}(x,y) = n_O - \frac{1}{2} n_O^3 R_{11} E^2(x,y) \qquad (4.12c)$$

$$n_{O'}(x,y) = n_O - \frac{1}{2} n_O^3 R_{12} E^2(x,y) \qquad (4.12d)$$

Finally, the refractive index for the parallel and perpendicular optical plane-wave orientations considered in experimentally characterizing and computationally simulating the electro-optically induced PLZT ceramic phase grating are computed.

$$n_{\parallel}(x,y) = n_{O'}(x,y) \qquad (4.13a)$$

$$n_{\perp}(x,y) = n_{e''}(x,y,\theta\ (x,y)) \qquad (4.13b)$$

$$\frac{1}{n_{e''}^2(\theta\ (x,y))} = \frac{\cos^2(\theta\ (x,y))}{n_{O'}^2(x,y)} + \frac{\sin^2(\theta\ (x,y))}{n_{e'}^2(x,y)} \qquad (4.13c)$$

Having computed the refractive index profile induced electro-optically within the transparent PLZT ceramic wafer, the phase delays experienced by parallel- and perpendicularly-oriented optical plane waves due to the intrinsic ITO electrode grating and the induced refractive index grating profile within the PLZT wafer can be expressed.

$$\Delta\phi_{||}(x) = \int_0^{d_{plzt}} n_{||}(x,y)dy \qquad (4.14a)$$

$$\Delta\phi_{\perp}(x) = \int_0^{d_{plzt}} n_{\perp}(x,y)dy \qquad (4.14b)$$

$$\Delta\phi_{ITO}(x) = \begin{cases} n_{air}\, d_{ITO} & 0 \le x \le b/4 \\ n_{ITO}\, d_{ITO} & b/4 \le x \le 3b/4 \\ n_{air}\, d_{ITO} & 3b/4 \le x \le b \end{cases} \qquad (4.14c)$$

The optical plane waves emerging from the electro-optic PLZT/ITO phase grating are expressed in terms of the computed phase delays.

$$E_{||}(x) = ce^{-j\frac{2\pi}{\lambda}[\Delta\phi_{||}(x) + \Delta\phi_{ITO}(x)]} \qquad (4.15a)$$

$$E_{\perp}(x) = ce^{-j\frac{2\pi}{\lambda}[\Delta\phi_{\perp}(x) + \Delta\phi_{ITO}(x)]} \qquad (4.15b)$$

$$E_{ITO}(x) = ce^{-j\frac{2\pi}{\lambda}[\Delta\phi_{ITO}(x)]} \qquad (4.15c)$$

The far-field diffraction pattern induced by the electro-optic PLZT/ITO phase grating is computed as a Fourier transform of the PLZT/ITO phase grating's illuminated aperture.

$$E_{ITO}^{FAR}(X) = \int_{-L}^{L} E_{ITO} e^{jkXx/R} dx \qquad (4.16a)$$

$$E_{||}^{FAR}(X) = \int_{-L}^{L} E_{||} e^{jkXx/R} dx \qquad (4.16b)$$

$$E_{\perp}^{FAR}(X) = \int_{-L}^{L} E_{\perp} e^{jkXx/R} dx \qquad (4.16c)$$

5. Simulation Results

The theoretical model characterizing the transmitted Fresnel diffraction patterns of the polycrystalline PLZT/ITO ceramic electro-optic phase grating under the sequence of applied voltages was implemented. The simulation results obtained agree with the experimentally-recorded Fresnel diffraction patterns corresponding to a plane-wave source beam with an electric-field vector oriented perpendicular to the ITO electrode grating. With zero applied voltage, the simulation computes the Fresnel diffraction pattern due to the intrinsic transparent ITO electrode phase grating (Figure 5.1). Simulation results featured in Figure 5.2 of Fresnel diffraction patterns at applied voltages confirm the mode features displayed by the experimentally-recorded diffraction patterns. The simulation confirms a zero mode switch-off voltage of 140V. Simulation results featured in Figure 5.3 for higher-order modes in the Fresnel diffraction patterns under applied voltage confirm the behavior illustrated in the experimentally-recorded higher-order mode diffraction patterns.

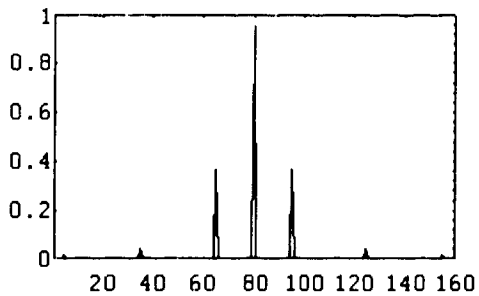

Figure 5.1 Transmitted Fresnel diffraction pattern due to intrinsic ITO electrode phase grating

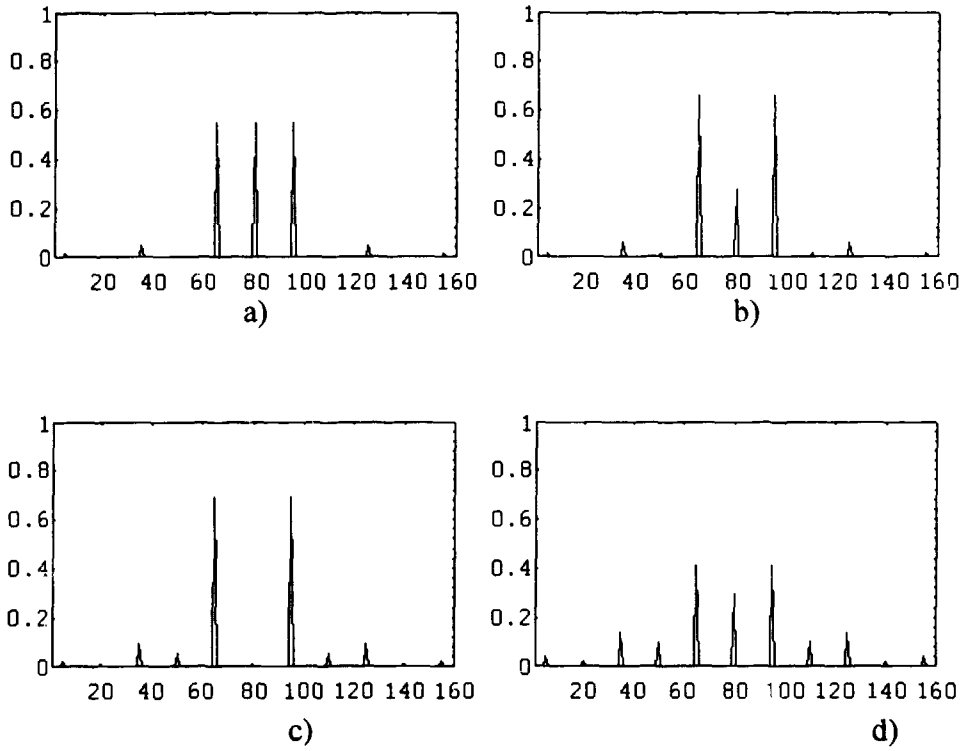

Figure 5.2 Transmitted Fresnel diffraction pattern due to induced electro-optic PLZT/ITO phase grating for perpendicular polarization :
a) v=75V, b) Vv100V, c) v=140V, d) v=175V.

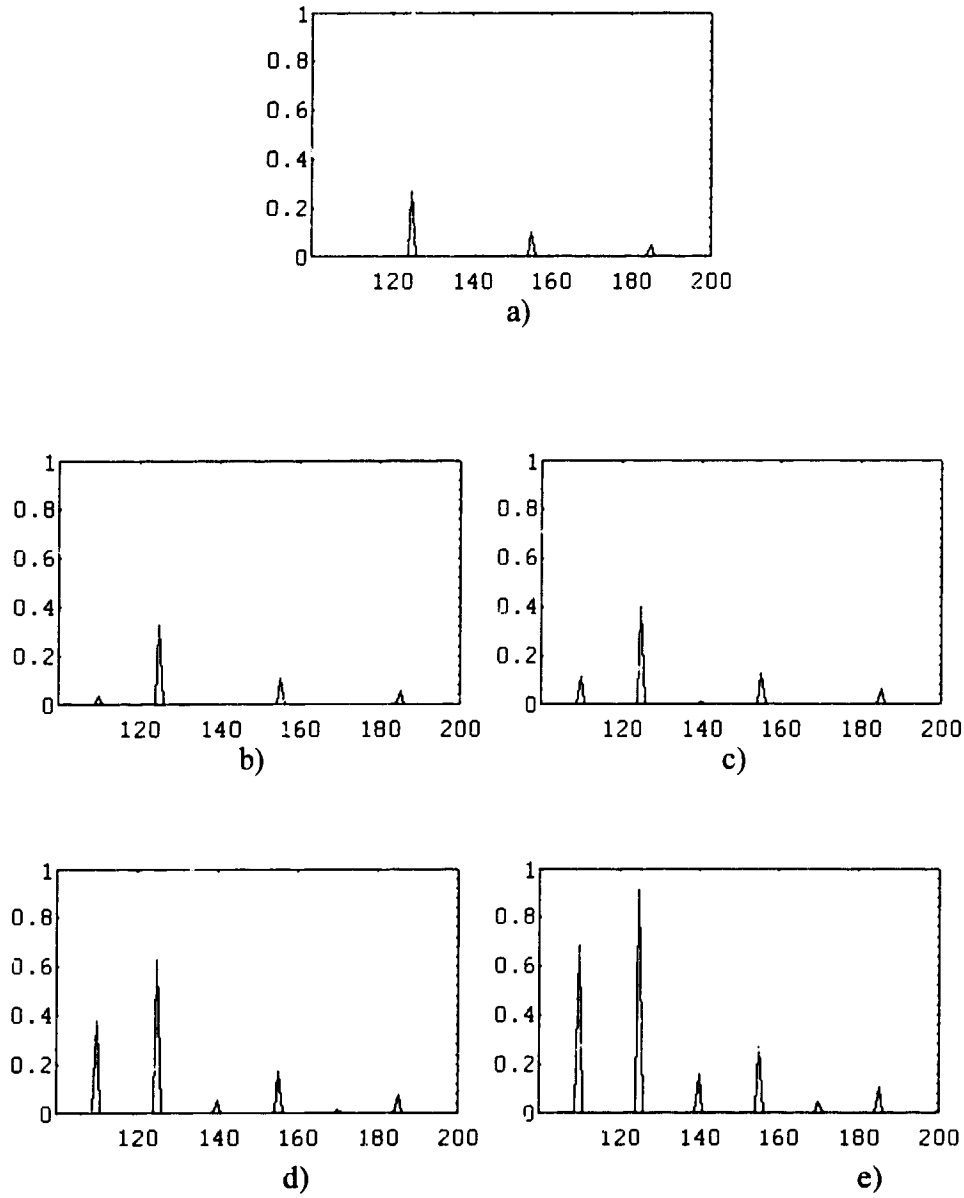

Figure 5.3 Transmitted Fresnel diffraction pattern due to induced electro-optic PLZT/ITO phase grating for perpendicular polarization - 2nd-and higher-order modes :
a) intrinsic ITO electrode phase grating (i.e., v=0V)
b) v=75V, c) v=100V, d) v=140V, e) v=175V.

The simulation results of the Fresnel diffraction patterns corresponding to a plane-wave source beam with an electric-field vector oriented parallel to the ITO electrode grating confirm the insignificance of the contribution of the electro-optically induced phase grating within the PLZT wafer to the Fresnel diffraction pattern experimentally observed for a parallel orientation (Figure 5.4). The simulation results illustrate the dominance of the diagonal Kerr coefficients in establishing electro-optically-induced diffraction patterns. The diagonal Kerr coefficients are responsible for the diffraction efficiency documented for the optical beams with perpendicular polarization while the off-diagonal Kerr coefficients determine the diffraction patterns seen for the optical beams with parallel polarization. The simulation results confirm the experimental observation that coupling the electric field through the diagonal Kerr coefficients is preferable in the design of electro-optically reconfigurable index profile elements. The use of ground planes in previously reported electro-optic diffractive devices tends to produce fields normal to the PLZT wafer surface and as such promotes electric field coupling through the less efficient off-diagonal Kerr coefficients of the quadratic electro-optic tensor. The elimination of ground planes and the use of transparent electrodes should dramatically improve the performance of the previously reported electro-optic PLZT ceramic diffraction devices.

The polycrystalline PLZT/ITO ceramic electro-optic phase grating preserves the polarization of the incident optical plane wave, but its electro-optic reconfiguration is polarization sensitive. The polarization sensitivity of the electro-optic PLZT/ITO phase grating coupled with the on/off switching of the zero-order transmitted mode can be utilized to produce a continuously variable polarization filter.

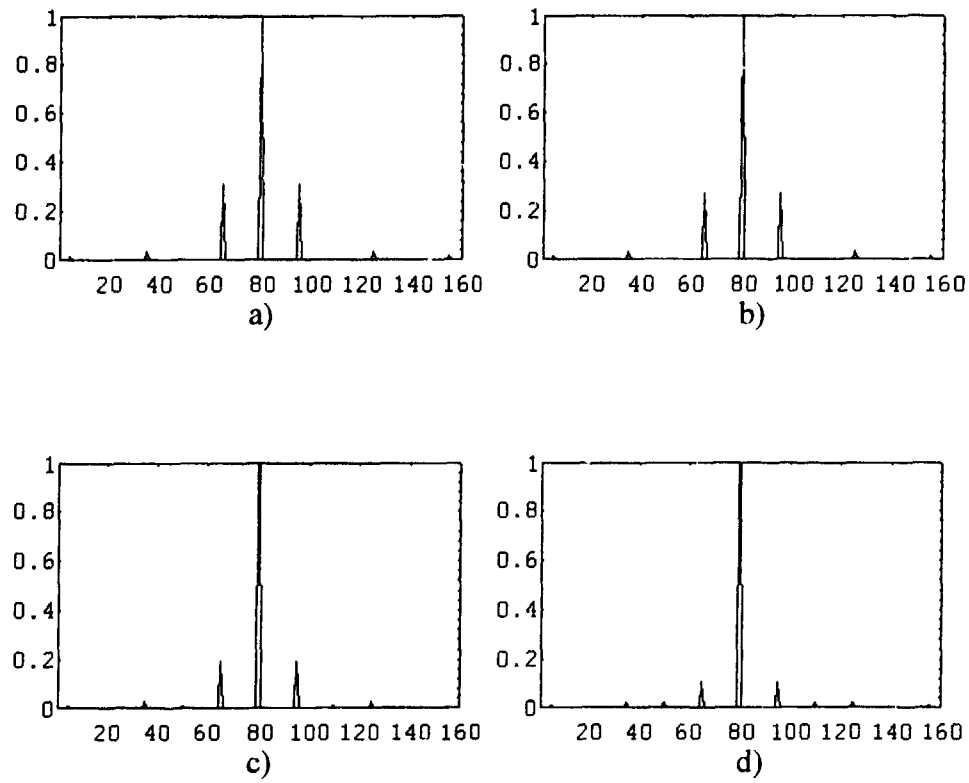

Figure 5.4 Transmitted Fresnel diffraction pattern due to induced electro-optic PLZT/ITO phase grating for parallel polarization :
a) v=75V, b) v=100V, c) v=140V, d) v=175V.

The typical relative magnitudes of the boundary-value coefficients are illustrated by those computed for simulation of an applied voltage of 140V (Figure 5.5). The steep, monotonic decline in the magnitude of the boundary coefficients and the relatively simple index ellipsoid manipulations inherent to the quadratic PLZT electro-optic tensor allow for accurate and tractable device simulation in the design of electro-optically reconfigurable index profile diffractive elements. The intrinsic optical isotropy of quadratic PLZT ceramic increases flexibility in device design and simplifies the fabrication process relative to intrinsically birefringent electro-optic materials with electro-optic tensors that induce complicated index ellipsoid orientations and device layout constraints such as lithium niobate.

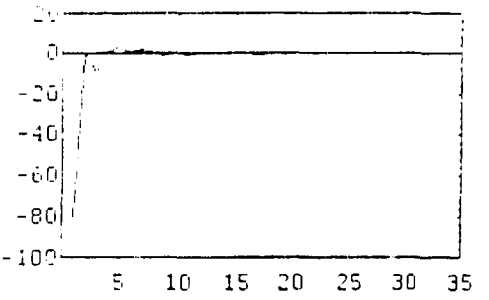

Figure 5.5 Computed boundary coefficients for v = 140V.

The typical profile of the components of the applied electric field within the PLZT ceramic wafer are illustrated by those computed for the simulation of an applied voltage of 140V (Figure 5.6).

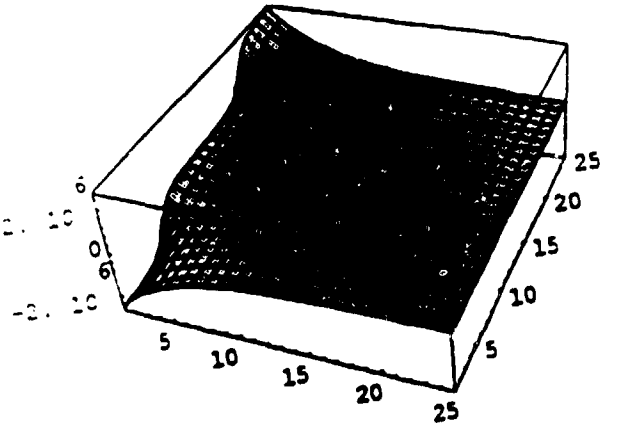

a)

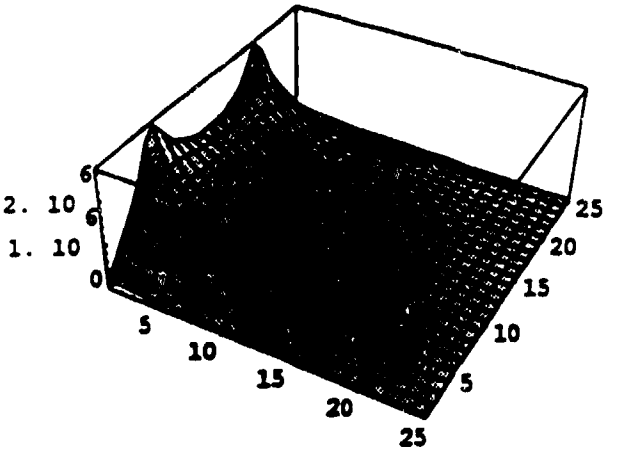

b)

Figure 5.6 Computed electric fields in PLZT ceramic wafer :

a) magnitude of x - component

b) magnitude of y - component.

The phase delays experienced by parallel- and perpendicularly-oriented optical plane waves are illustrated for the sequence of applied voltages utilized in the experimentally-recorded Fresnel diffraction patterns (Figure 5.7).

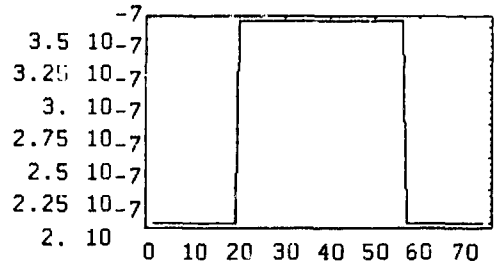

a)

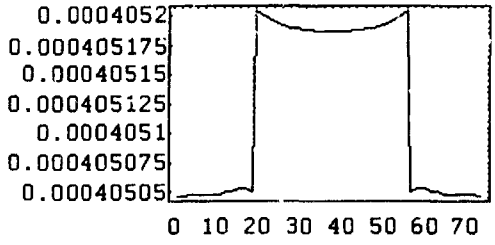

b)

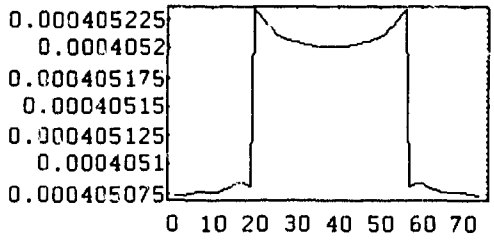

c)

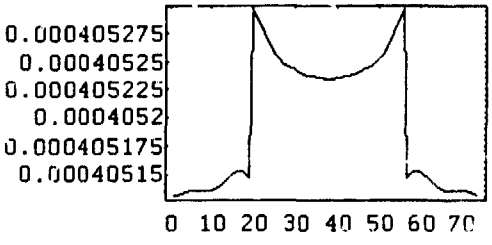

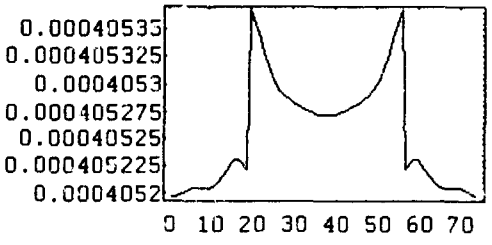

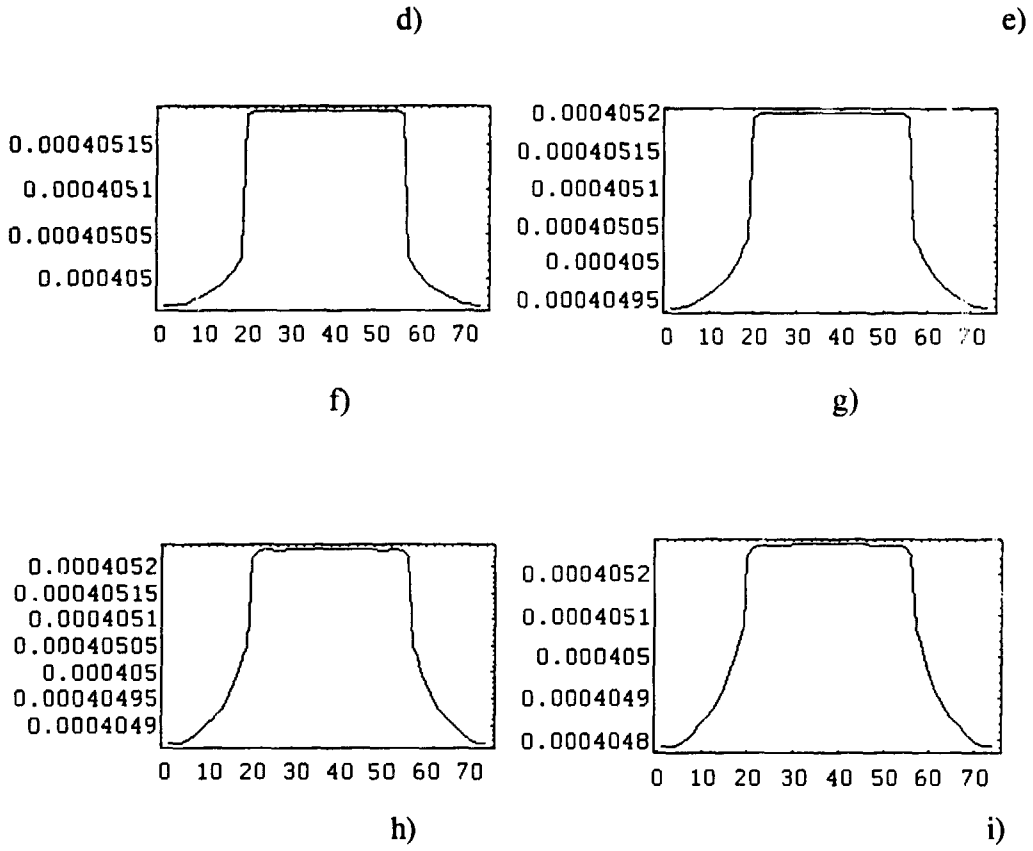

Figure 5.7 Phase delay due to induced PLZT/ITO phase grating for
a) intrinsic ITO electrode phase grating (i.e., v=0V) ;
parallel polarization : b) v=75V, c) v=100V, d) v=140V, e) v=175V;
perpendicular polarization : f) v=75V, g) v=100V, h) v=140V, i)v=175V.

Simulations of the Fresnel diffraction patterns under the sequence of applied voltages for an optical plane wave oriented perpendicular to the ITO electrode grating were corrected to eliminate the contribution of the intrinsic ITO electrode phase grating to the diffraction patterns (Figure 5.8). The electro-optically induced phase grating for perpendicular orientation exhibited diffraction patterns in the same order of magnitude as that produced by the intrinsic ITO electrode phase grating. Refractive index compensating thin films could be utilized to produce reconfigurable index profile diffractive elements which possess an intrinsically-uniform refractive index profile thereby eliminating intrinsic diffraction modes.

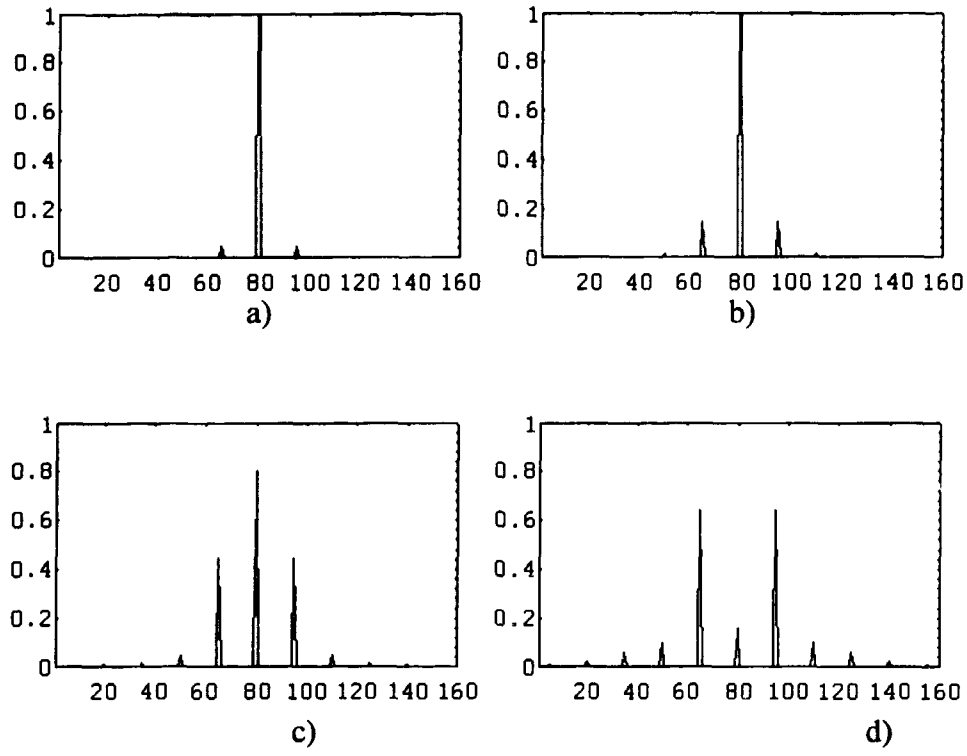

Figure 5.8 Transmitted Fresnel diffraction pattern due to induced electro-optic PLZT/ITO phase grating for perpendicular polarization - compensated for intrinsic ITO electrode phase grating : a) v=75V, b) v=100V, c) v=140V, d) v=175V.

6. Conclusions

The experimental evaluation and model simulation of our polycrystalline PLZT/ITO ceramic electro-optic phase grating demonstrates the performance improvements and advantages of our design. The utilization of quadratic PLZT compositions reduces the required driving voltages compared to linear electro-optic materials. The 100% modulation voltage for the zeroeth diffraction mode is significantly lower than reported values for all previous non-waveguide-based devices utilizing lithium niobate or PLZT electro-optic materials. Transparent ITO electrodes produce a phase-only grating that can be operated in either transmissive or reflective mode. The electro-optic tensor is intrinsically isotropic and so provides fabrication and alignment flexibility over lithium niobate. PLZT is intrinsically non-birefringent and so allows for flexible orientation of incident beam polarization. In

addition, PLZT ceramics exhibit minimal photorefractive optical damage. The device possesses a large angle of incidence, and large apertures are conveniently produced.

The experimental confirmation of our theoretical model implies some basic rules for the design and fabrication of electro-optic diffractive devices based on quadratic PLZT ceramic. First, the structure of the device should be such that the electric fields are coupled through the diagonal Kerr coefficients to produce the most efficient index profile variations. Second, design and fabrication of the structure should be guided by the requisite parallel orientation of the optical beam polarization and the electric field.

Microelectronic architectures and fabrication processes are utilizing electro-optic PLZT based devices. Epitaxial PLZT thin-film, total-internal-reflection (TIR) switches that operate at voltages compatible with microelectronics have been reported [22]. The PLZT TIR switch as well as waveguide-based lithium-niobate diffractive schemes [31] suggests promising performance and applications for PLZT ceramic diffractive devices in waveguide-based optical-interconnection architectures. PLZT modulator-based free-space optical interconnects and processing has been extensively implemented and evaluated in the context of smart pixel integrated optoelectronics [32-37]. The PLZT modulators are operated in transmissive and reflective modes within the architecture. A natural extension to the smart pixel optoelectronic architecture would be to incorporate deflection- and/or scanning-interconnect elements to implement optical pathways and facilitate post-fabrication alignment and failure recovery. PLZT/ITO electro-optically reconfigurable index profile diffractive structures provide promising candidates for the micro-optic deflection and/or scanning elements. Scaling investigations of the polycrystalline PLZT/ITO electro-optic phase grating are underway. We are also investigating the utility of other PLZT/ITO electro-optic diffractive structures as possible micro-optic reconfigurable index profile elements for optical-interconnection architectures.

References

1. S.C. Esener, T.J. Drabik, C.C. Guest, and M.R. Feldman, "Comparison between optical and electrical interconnects based on power and speed considerations," Applied Optics, Vol. 27, No. 9, pp. 1742-1751, 1988.

2. S.C. Esener, T.J. Drabik, C.C. Guest, and M.R. Feldman, "Comparison between electrical and free space optical interconnects for grain processor arrays based on interconnect density capabilities," Applied Optics, Vol. 28, No. 18, pp. 3820-3829, 1989.

3. S.C. Esener, F. Kiamilev, S. Krishnakumar, P. Marchand, and S.H. Lee, "Performance comparison between optoelectronic and VLSI multi-stage interconnection networks," IEEE Journal of Lightwave Technology, Vol. 9, No. 12, pp. 197-220, 1991.

4. S.C. Esener, F. Kiamilev, S. Krishnakumar, and P. Marchand, "Grain-size considerations for optoelectronic multi-stage interconnection networks," Applied Optics, Vol. 31, No. 26, pp. 5480-5507, 1992.

5. K.H. Brenner and F. Sauer, "Diffractive-reflective optical interconnects," Applied Optics, Vol. 27, No. 20, pp. 4251-4254, 1988.

6. J. Jahns, Y.H. Lee, C.A. Burrus Jr., and J.L. Jewell, "Optical interconnects using top-surface-emitting microlasers and planer optics," Applied Optics, Vol. 31, No. 5, pp. 592-597, 1992.

7. F. Lin, E.M. Strzelecki, and T. Jannson, "Optical multiplanar VLSI interconnects based on multiplexed waveguide holograms," Applied Optics, Vol. 29, No. 8, pp. 1126-1133, 1990.

8. K. Rastani and W.M. Hubbard, "Large interconnects in photorefractives: grating erasure problem and a proposed solution," Applied Optics, Vol. 31, No. 5, pp. 598-605, 1992.

9. B. Dhoedt, P.D. Dobbelaere, L. Buydens, R. Baets, and B. Houssay, "Optical free space board to board interconnects : options for optical pathways," Applied Optics, Vol. 31, No. 26, pp. 5508-5516, 1992.

10. M.R. Wang, G.J. Sonek, R.T. Chen, and T. Jannson, "Large fanout optical interconnects using thick holographic gratings and substrate wave propagation," Applied Optics, Vol. 31, No. 2, pp. 236-249, 1992.

11. K. Rastani and W.M. Hubbard, "Alignment and fabrication tolerances of planar gratings for board-to-board optical interconnects," Applied Optics, Vol. 31, No. 23, pp. 4863-4870, 1992.

12. Y. Yamanaka, K. Yoshihara, I. Ogura, T. Numai, K. Kasahara, and Y. Ono, "Free space optical bus using cascaded vertical to surface transmission electrophotonic devices," Applied Optics, Vol. 31, No. 23, pp. 4676-4681, 1992.

13. R.P. Bocker, G.M. Meana, M.A. Monahan, G.C. Mooradian, W.E Richards, and H.F. Taylor, "A large aperture electro-optic diffraction modulator," Journal of Applied Physics, Vol. 50, No. 11, pp. 6691-6693, 1979.

14. J.M. Hammer, "Digital electro-optic grating deflector and modulator," Applied Physics Letters, Vol. 18, No. 4, pp. 147-149, 1971.

15. R.A. Meyer, "Optical beam steering using a multichannel lithium tantalate crystal," Applied Optics, Vol. 11, No. 3, pp. 613-616, 1972.

16. J.N. Polky and J.H. Harris, "Interdigital electro-optic thin film modulator," Applied Physics Letters, Vol. 21, No. 7, pp. 307-309, 1972.

17. M. Hammer, D.J. Channin, and M.T. Duffy, "Fast electro-optic waveguide deflector modulator," Applied Physics Letters, Vol. 23, No. 4, pp. 176-177, 1973.

18. T. Motoki, "Low voltage optical modulator using electro-optically induced phase gratings," Applied Optics, Vol. 12, No. 7, pp. 1472-1476, 1973.

19. W.E. Martin, "A new waveguide switch/modulator for integrated optics," Applied Physics Letters, Vol. 26, No. 10, pp. 562-564, 1975.

20. H. Sato and K. Toda, "A new electrically controllable diffraction grating using polarization reflection," Journal of Applied Physics, Vol. 47, No. 9, pp. 4031-4032, 1976.

21. T. Kawaguchi, H. Adachi, K. Setsune, O. Yamazaki, and K. Wasa, "PLZT thin film waveguides," Applied Optics, Vol. 23, No. 13, pp. 2187-2191, 1984.

22. T. Kawaguchi, H. Adachi, K. Setsune, O. Yamazaki, and K. Wasa, "Optical TIR switches using PLZT thin-film waveguides on sapphire," Journal of Lightwave Technology, Vol. LT-2, No. 5, pp. 710-714, 1984.

23. H. Sato, T. Tatebayashi, T. Yamamoto, and K. Hayashi, "Electro-optic lens composed of transparent electrodes on PLZT ceramic towards optoelectronic devices," Optics in Complex Systems, SPIE Vol. 1319, pp. 493-494, 1990.

24. H. Sato, T. Yamamoto, and T. Tatebayashi, "Electro-optic variable focal-length lens using PLZT ceramic," Applied Optics, Vol. 30, No. 34, pp. 5049-5055, 1991.

25. H. Sato, T. Yamamoto, and T. Tatebayashi, "Dual focal point electro-optic lens with a Fresnel-zone plate on a PLZT ceramic," Applied Optics, Vol. 31, No. 15, pp. 2770-2775, 1992.

26. R.C. Buchanan (ed.), Ceramic Materials for Electronics, Haertling G.H. (Chapter 3), Marcel Dekker, New York, 1986.

27. L.M. Levinson (ed.), Electronic Ceramics, Haertling G.H. (Chapter 7), Marcel Dekker, New York, 1988.

28. A.J. Moulson and J.M. Herbert, Electroceramics: Materials-Properties-Applications, Chapman and Hall, New York, 1990.

29. A. Yariv and P. Yeh, Optical Waves in Crystals, Wiley, New York, 1984.

30. J.F. Nye, Physical Properties of Crystals, Clarendon Press, Oxford, 1957.

31. R.T. Chen, D. Robinson, H. Lu, M.R. Wang, and T Jannson, "Reconfigurable optical interconnection network for multimode optical fiber sensor arrays," Optical Engineering, Vol. 30, No. 5, pp. 1098-1106, 1992.

32. S.C. Esener, T.J. Drabik, M.A. Title, and S.H. Lee, "Two-dimensional silicon/PLZT spatial light modulators: Design Considerations and Technology," Optical Engineering, Vol. 25, No. 2, pp. 250-260, 1986.

33. S.C. Esener, J.H. Wang, T.J. Drabik, M.A. Title, and S.H. Lee, "One-dimensional silicon/PLZT spatial light modulators," Optical Engineering, Vol. 26, No. 5, pp. 406-413, 1987.

34. S.C. Esener, "Silicon-based smart spatial light modulators: technology and applications to parallel computers," Digital Optical Computing, SPIE Critical Reviews Vol. CR35, pp. 100-125, 1990.

35. S.C. Esener, F. Kiamilev, V.H. Ozguz, and S.H. Lee, "Programmable optoelectronic multiprocessor systems," Digital Optical Computing, SPIE Critical Reviews Vol. CR35, pp. 197-220, 1990.

36. S.C. Esener, J.H. Wang, A. Ersen, S. Krishnakumar, V.H. Ozguz, C. Fan, and S.H. Lee, "Design issues and development of monolithic silicon/PLZT integrated technologies for smart spatial light modulators," Applied Optics, Vol. 31, No. 20, pp. 3950-3965, 1992.

37. S.C. Esener, F. Kiamilev, R. Paturi, Y. Fainman, P. Mercier, C.C. Guest, and S.H. Lee, "Programmable optoelectronic multiprocessors and their comparison with symbolic substitution for digital optical computing," Applied Optics, Vol. 27, No. 20, pp. 4251-4254, 1988.

MISSION

OF

ROME LABORATORY

Mission. The mission of Rome Laboratory is to advance the science and technologies of command, control, communications and intelligence and to transition them into systems to meet customer needs. To achieve this, Rome Lab:

a. Conducts vigorous research, development and test programs in all applicable technologies;

b. Transitions technology to current and future systems to improve operational capability, readiness, and supportability;

c. Provides a full range of technical support to Air Force Materiel Command product centers and other Air Force organizations;

d. Promotes transfer of technology to the private sector;

e. Maintains leading edge technological expertise in the areas of surveillance, communications, command and control, intelligence, reliability science, electro-magnetic technology, photonics, signal processing, and computational science.

The thrust areas of technical competence include: Surveillance, Communications, Command and Control, Intelligence, Signal Processing, Computer Science and Technology, Electromagnetic Technology, Photonics and Reliability Sciences.